

■ Title

The CANadian NIRISS Unbiased Cluster Survey (CANUCS)

■ Authors

NIRISS GTO *High-redshift galaxies and galaxy evolution* Working Group:
Willott, Abraham, Albert, Bradac, Brammer, Chayer, Dixon, Doyon, Dupuis, Ferrarese, Goodfrooij, Hutchings, Martel, Ravindranath, Sawicki

■ Abstract

We propose a slitless spectroscopy and imaging survey of five massive galaxy cluster and ten parallel fields using the NIRISS low-resolution grisms, NIRC*am* imaging and NIR*Spec* multi-object spectroscopy. This survey will yield spectra of 10,000 and imaging of 100,000 distant galaxies, with the primary goal of understanding the evolution of low mass galaxies across cosmic time. The resolved emission line maps and line ratios for many galaxies, some at resolution of ~ 100 pc, will enable determining the spatial distribution of star formation, dust and metals. Other science goals include the detection and characterization of galaxies within the reionization epoch, using multiply-imaged lensed galaxies to constrain cluster mass distributions and dark matter substructure, and understanding star-formation suppression in the most massive galaxy clusters.

Table 1: Summary of Observations per Cluster

Instrument	Mode	Prime?	#Configs	Exp. Time (h)	Tot. Time (h)
NIRISS	WFSS	Prime	6	21.2	27.33
NIRC <i>am</i>	Image	Prime	3	6.3	8.88
NIR <i>Spec</i>	MOS	Prime	2	1.9	3.64
NIRC <i>am</i>	Image	Parallel	7	21.2	–
NIRISS	WFSS	Parallel	3	6.3	–

Table 1 notes:

Prime observations are all centred on the lensing clusters.

WFSS mode includes some fraction of time of NIRISS direct imaging.

Tot. Time is the total time required per cluster including direct and indirect overheads (based on APT v25.0).

The total time request for this project is 199 hrs.

Time request breakdown by prime instrument: NIRISS 137 hrs, NIRC*am* 44 hrs, NIR*Spec* 18 hrs.

■ Scientific Justification

1. The Evolution of Dwarf Galaxies

Dwarf galaxies (stellar mass $M_* < 10^9 M_\odot$) are the most numerous star-forming galaxies in the Universe. Living primarily in low mass halos in sparse environments, their evolution depends on the interplay between gas accretion from gravitational infall and expulsion by stellar evolution induced outflows. The proposed NIRISS grism and NIRCам imaging observations will measure physical properties for 3000 dwarf galaxies at $z > 1$ (Fig. 1). This will provide a picture of galaxies across cosmic time to be compared with simulations to determine the physical processes that shape how galaxies evolved. State-of-the-art hydrodynamical simulations, such as Illustris (Nelson et al. 2015), do not match the observed stellar mass function at $M_* < 10^{9.5} M_\odot$, because of uncertainty in stellar feedback in low mass halos (Genel et al. 2014) and require observations with *JWST* to make further progress.

We will measure redshift, stellar mass, star formation rate, dust extinction and metallicity. Stellar masses and star-formation histories will come from fitting the full optical to $5\mu\text{m}$ SED, including emission lines. Instantaneous star formation rate (SFR) and dust extinction will come from emission lines. For gas-phase metallicities the ratios of the [OII], [NeIII], $\text{H}\gamma$, $\text{H}\beta$ and [OIII] lines give a reddening-independent oxygen abundance, O/H. Using the GR150 grisms and filters F115W, F150W and F200W, the key lines are obtained for galaxies at $1.72 < z < 2.32$ and $2.61 < z < 3.35$, essentially giving us samples at $z \sim 2$ and $z \sim 3$ (Fig. 1). About half of the 3000 dwarf galaxies at $z > 1$ lie at redshifts appropriate for a metallicity measurement, generating the largest sample at $z > 1.5$ by a factor of ≈ 10 (c.f. Sanders et al. 2015). At least 1250 galaxy metallicity measurements are required to split the sample into 5 bins of each variable z, M_*, SFR with > 10 galaxies per bin.

Currently, the mass-metallicity (M-Z) relation has been observed out to $z = 2 - 2.5$ (Steidel et al. 2014; Sanders et al. 2015), but only probing the high-mass ($> 10^9 M_\odot$) end. The high-mass M-Z relation at high redshifts is offset from the $z = 0$ relation defined using SDSS galaxies. The unknown low-mass end is of special interest because that is where the effects of stellar feedback are expected to be the greatest and simulations most uncertain as to whether galaxies are able to retain most of their metals (Ma et al. 2016). We will determine this relation (and associated correlation with SFR (Fundamental Metallicity Relation; Mannucci et al. 2010) and compare with theoretical models such as the FIRE cosmological zoom-in simulations (Ma et al. 2016).

The proposed NIRISS observations in lensing fields will also generate a uniquely large sample (> 100) of *spatially-resolved* (at scales 100 pc) dwarf galaxy metallicities. Use of gravitational lensing is crucial to dissect low luminosity, intrinsically small galaxies and probe prior star formation, outflows, gravitational infall and dynamical evolution. Only a limited number of high-redshift galaxies have been observed with the WFC3 grisms (Jones et al. 2015; Wang et al. 2016; Fig. 3) and NIRISS will far outperform previous work.

We will also carry out a ground-breaking study of extreme emission line galaxy (EELG) evolution over the redshift range $1 < z < 8$. Emission line strengths rise rapidly with redshift (Fumagalli et al. 2012) and inversely with mass so that there is a large high-redshift population of EELGs (van der Wel et al. 2011; Stark et al. 2013; Smit et al. 2014). With NIRISS WFSS we identify EELGs up to $z = 3.5$ by their [OIII] emission and with the NIRCам medium band survey in the parallel fields extend this to $z = 8$. Galaxy properties (emission line ratios, evolutionary state, SFR clumpiness, etc.) will be used to determine the physical reasons for the strong lines over an unprecedented redshift range.

Moreover, we will measure the evolving $H\alpha$ luminosity function as a proxy for the global SFR function. Including lensing we will be sensitive to $SFR \sim 0.01 M_{\odot} \text{yr}^{-1}$, a regime where the stochastic nature of star formation is important (Dominguez et al. 2015). Comparisons of dust-corrected UV luminosity, $H\alpha$ luminosity and stellar mass will determine where these low-mass galaxies lie on the SFR–stellar-mass main sequence, their recent star formation history and a detailed comparison with theoretical models of bursts in SFR in low mass galaxies.

Furthermore, for well-resolved galaxies we will study when and where stars formed and where the dust is located. We will determine the clumpiness of star formation to understand why high-redshift disks appear to have more massive (10^7 to $10^8 M_{\odot}$) star-forming clumps than in the local universe (Elmegreen & Elmegreen 2005; Genzel et al. 2008; Guo et al. 2012). The NIRISS WFSS observations of lensing clusters will be unique for these studies because they enable 2D emission-line mapping of about 50 giant lensed arcs, with high spatial resolution to resolve the sub-structures within high- z galaxy disks.

2. Galaxies in the Reionization Epoch

Our NIRISS observations will identify a large sample of galaxies in the reionization epoch at redshifts $z > 6$. Cosmological reionization is an important event in the history of the Universe, marking the rise of the UV background, likely due to the formation of the first galaxies. By tracing the evolution of the neutral fraction of hydrogen over space and time we can infer details of the sources responsible for reionization, most likely galaxies too faint to be individually studied.

One of the most promising ways to probe evolution in the IGM neutral fraction is by its effect on absorption of Lyman- α emission lines from galaxies. The fraction of galaxies with Lyman- α emission is found to increase from about 30% at $z = 4$ to 40% at $z = 6$, probably due to a lower dust content at higher redshifts, and then decrease sharply at higher redshifts (Schenker et al. 2014). This high redshift decline in Lyman- α is believed to be due to a higher IGM neutral fraction within the reionization epoch. But current samples are small and ground-based studies have uncertain completeness due to atmospheric attenuation and sky emission. Also, it is known that Lyman- α is emitted over a more extended region than the UV continuum due to resonant scattering off neutral gas in the outer regions of the galaxy, and this causes uncertainty in slit-based Lyman- α equivalent widths.

NIRISS will be unique in its ability to enable blind selection of $z > 7$ galaxies in the grism data as spectra showing a break (e.g. Fig. 4 and 5) and/or an emission line. The grism spectra will therefore be crucial to determine accurate redshifts and Lyman- α equivalent widths. NIRISS simulations and observations with WFC3 (Schmidt et al. 2016) show that rest-frame equivalent widths down to $\approx 10 \text{ \AA}$ can be detected with grism spectra and this is competitive with the limits of ground-based spectroscopy. $z > 5$ galaxies selected with HST, NIRISS and NIRCам broad-band imaging will be targeted with NIRSpec to get emission lines at redshifts not covered by the NIRISS wavelength range.

With a sample of ~ 200 galaxies at $z > 6$ we will determine the Lyman- α observability as a function of redshift and UV luminosity into the reionization epoch. Assuming some fraction of sources are clustered we may also be able to investigate whether the Lyman- α observability is clustered and how it depends upon galaxy overdensity. The observational results will be compared to reionization models (Gnedin 2014; Chardin et al. 2015) to determine not only the global neutral fraction but also the patchiness of reionization.

We will study correlations between Lyman- α and other properties, such as continuum morphology. The merger fraction among LAEs and their relation to $EW(\text{Lyman-}\alpha)$ will be quantified

using commonly used indicators like the Gini coefficients, M20, Asymmetry, etc. The separation between the individual components of a merger will also be measured because there have been studies showing an anti-correlation between separation and $\text{EW}(\text{Lyman-}\alpha)$. We will use ellipticity measurements to look for trends with $\text{EW}(\text{Lyman-}\alpha)$ and $L(\text{Lyman-}\alpha)$ that is expected if the Lyman- α emission is preferentially in face-on disks.

3. Massive Clusters and Dark Matter

The targeting of massive galaxy clusters allows us to address several important science questions. The clusters are the highest density peaks in the cosmic matter distribution where spectacular galaxy transformations occur. With the proposed imaging we will identify the distribution of the intracluster light and globular cluster population to reveal previous stripping from galaxies that fell into the cluster. With multi-band imaging from the core to beyond the virial radius we will determine how the cluster environment affects galaxy evolution (Fig. 6). For the two higher redshift clusters ($z > 0.5$), the $\text{H}\alpha$ line is located in the F115W filter bandpass, so we will be able to determine SFR for galaxies and confirm cluster membership for extremely low luminosity galaxies.

Via modelling of strong gravitational lensing we will determine the dark matter distribution. With the great improvement in the number of multiply-imaged systems with redshifts measured by NIRISS and NIRSpec (estimated at ≈ 100 per cluster based on Frontier Fields analysis and our simulations) we will fit highly accurate lensing models and map out the 2D mass distribution within the cluster, determining the halo mass function and the spatial distribution of the substructure (e.g. Jauzac et al. 2016).

Strong gravitational lensing enables measuring the geometry of the universe. By measuring accurate positions and redshifts of multiply-imaged galaxies at different redshifts one can constrain cosmological parameters (Gilmore & Natarajan 2009; Jullo et al. 2010). We will improve on previous work in three main ways: i) the very large number of multiply-imaged galaxies allows tests of data consistency and statistical removal of outliers; ii) making use of lensed galaxy pairs at different redshifts along similar lines-of-sight will also help to reduce the effect of uncertain lensing mass distribution; iii) identify and model the extra lensing by mass along the line-of-sight.

4. Additional Science Goals

There are other science goals that we will pursue with our program. These are briefly mentioned below, but have all been scoped in considerably greater detail.

Galactic Science With the NIRISS grisms we can detect and categorize faint objects with broad spectral features like cool M, L, T, and Y dwarfs and free-floating Jovian planets.

Quenching We will obtain high S/N spectra of passive and recently quenched galaxies at $z < 4$ to study how potential quenching mechanisms of AGN, morphological and halo quenching affect galaxies as a function of mass.

Merger Rate With accurate redshifts from grism spectroscopy ($\delta z = 0.003 \times (1+z)$; Momcheva et al. 2016), we will determine when observed pairs are true physical pairs and not simply projection effects and determine evolution in the merger rate.

Environments Grism redshifts will determine which galaxies are located in groups or clusters so we can see how environment affects galaxy evolution.

Transients As exemplified by recent Frontier Fields observations, deep observations in lensing clusters will sometimes pick up transient sources, including very high-mass progenitor core-collapse supernovae up to very high redshift.

■ Description of the Observations

1. Targets

This program will observe 5 massive galaxy cluster and parallel fields. The Scientific Justification highlights the unique science that can be done in these fields thanks to gravitational lensing. A minimum sample of 5 clusters is required for our science goals. This provides the required statistics for the number of background galaxies as detailed in Sections 1 and 2. Additionally 5 clusters are required to prevent cosmic variance becoming the limiting factor for the statistics, due to the reduced volume behind lensing clusters compared to the field. For example, for the number of galaxies expected in a redshift bin of size $\delta z = 0.5$ at redshift 3, cosmic variance exceeds the Poisson variance in typical lensing cluster NIRISS-sized fields (using the cosmic variance calculator of Trenti & Stiavelli 2008).

The five clusters listed in Table 2 have been selected based on i) high mass and large area with high magnification; ii) critical curves that fit within the NIRISS field; iii) > 10 degrees away from zodiacal plane for low background; iv) little area lost to bright stars; v) $z > 0.35$ to avoid contaminating light from ICL and cluster galaxies; vi) good data at other wavelengths, especially deep ACS optical for redshift and SED fitting.

Table 2: Target List.

Cluster	RA	DEC	Redshift	Survey	<i>JWST</i> Visibility Period
Abell 370	02:39:52.8	-01:34:36	0.375	HFF	24 Jul-16 Sep + 12 Dec-02 Feb
M0416.1-2403	04:16:09.4	-24:04:04	0.395	HFF	12 Aug-09 Nov + 27 Nov-22 Feb
M0417.5-1154	04:17:34.7	-11:54:32	0.443	RELICS	17 Aug-20 Oct + 26 Dec-24 Feb
M1149.6+2223	11:49:35.9	+22:23:55	0.543	HFF	19 Apr-15 Jun + 05 Dec-27 Jan
M1423.8+2404	14:23:47.8	+24:04:40	0.545	CLASH	13 May-24 Jul + 08 Jan-15 Mar

2. NIRISS Prime Observations

We will observe the cluster fields with NIRISS direct imaging and the two orthogonal R=150 grisms in three broad-band filters F115W, F150W and F200W to cover the wavelength range 1 to $2.2\mu\text{m}$. With a total grism exposure time of 6.4 hrs per filter we reach a significant increase in depth compared to previous work with *HST* opening up new parameter space in redshift, luminosity, stellar mass and star formation rate. The total exposure time per filter per grism is divided into 12 exposures of 945s each with small dithers between them. As part of the WFSS observing sequence we obtain 8 direct images per filter of 343s each, used to determine the flux, trace position and wavelength in the grism data.

Grism continuum sensitivity at 3σ per pixel is AB=26.4, 26.4, 26.0 in F115W, F150W, F200W. Emission line sensitivity at 3σ for an unresolved line is 1.7, 1.1, 0.9×10^{-18} erg s $^{-1}$ cm $^{-2}$ in F115W, F150W, F200W. Sensitivity limits for spatially-resolved information will be proportionately shallower due to the larger area over which flux is distributed. Direct imaging sensitivity is 10σ : F115W 28.0, F150W 28.1, F200W 28.3. Instrument overheads are 1.87 hrs, one large slew is 1800 s plus indirect overheads of 3.77 hrs gives total time per cluster of 27.33 hrs.

3. NIRCам Prime Observations

NIRCам LW photometry observations in three filters (F277W, F356W and F444W) of the NIRISS WFSS target fields are required to measure SEDs and better constrain redshift, stellar

mass and star-formation history. NIRCcam obtains SW and LW data at the same time, so we also get filters F090W, F150W and F200W. For NIRCcam we will use a larger dither size than NIRISS of $\approx 10''$ to provide imaging of the region just beyond the grism field to enable grism modelling of sources outside the field-of-view. 8 exposures of 945s each gives 10σ point source limiting magnitudes of F090W 28.2, F150W 28.6, F200W 28.8, F277W 28.6, F356W 28.7, F444W 28.1. Instrument overheads are 4886 s plus indirect overheads of 4411 s gives total time per cluster of 8.88 hrs.

4. NIRSpec Prime Observations

We will follow up the Prime NIRISS and NIRCcam observations with the NIRSpec Micro Shutter Array (MSA) to target galaxies for which NIRISS does not yield redshifts due to either contamination or a redshift with no emission lines in the NIRISS wavelength range ($5 < z < 7.3$). We will prioritize very high-redshift and multiply-imaged galaxies, some of which are already known based on existing imaging.

We use the R=100 prism as we are mostly interested in redshifts and line ratios and this mode gives a higher multiplex factor than the higher resolution gratings (multiple bands of targets across the detectors). We will use two MSA configurations offset over the gaps between MSA quadrants. Each configuration will be observed for 3480s total integration (3×1160 s exposures, nodding along the 3 shutter slitlet). The sensitivity (3σ per pixel at $3\mu\text{m}$) for compact galaxies observed in both configurations is 27.0 in the continuum and $0.6 \times 10^{-18} \text{ erg s}^{-1} \text{ cm}^{-2}$ for emission lines. Instrument overheads are 0.71 hrs, one large slew is 1800 s plus indirect overheads of 0.50 hrs gives total time per cluster of 3.64 hrs.

5. NIRCcam Parallel Observations

The two science goals for parallel NIRCcam data are: 1) To sample galaxies at 3 to 8 arcminutes (1.0 to 2.5 Mpc) from the cores to infall regions of massive strong-lensing clusters. Imaging with NIRCcam will allow galaxy shapes to be measured at these distances and compared with those nearer the cluster core to study the morphological transformation of galaxies as they fall into the cluster. 2) Extend the study of extreme emission line galaxies (EELGs) up to $z = 8$ by using Medium width bands that can be dominated by strong emission lines. An emission line at $z = 4$ with rest-frame equivalent width 200 \AA would make a perturbation to the Medium band photometry of between 50 and 25%.

In the LW arm of NIRCcam, we use the two Wide filters F277W and F444W plus five medium filters F300M, F335M, F360M, F410M and F480M, giving effectively 7 medium LW bands. The simultaneous NIRCcam SW filters required are F070W, F090W, F115W, F150W, F182M and F210M. The NIRCcam survey would reach magnitude limits (10σ , point source) of 28 to 29 in the six Wide filters and 27 to 28 in the seven Medium filters.

6. NIRISS Parallel Observations

The main science goal for parallel NIRISS data is to identify $7.3 < z < 9.5$ galaxies for the science discussed in Section 2 of the Scientific Justification. Use of the parallel fields will provide an increased area to find these galaxies which is important because such galaxies are rare. With 6.3 hrs on-source time per field only the F115W filter with both grisms will be used to attain similar depth to the main NIRISS observations on the cluster core. For the two highest redshift clusters, the $\text{H}\alpha$ line is in the F115W filter, aiding our study of galaxy transformations in cluster outskirts.

7. Scheduling and Co-ordination

This is a statistical study of five galaxy clusters so we wish to obtain all data in Cycle 1. There is no point in splitting the data between Cycles 1 and 2 and writing two sets of papers on each topic. However, we will write some early papers based on preliminary analysis of the first one or two clusters in order to give the community an early look at the capabilities of NIRISS for this type of science. The NIRSpec MOS observations will be follow-up of the NIRCам and NIRISS Prime observations, so it is required that the NIRCам and NIRISS be scheduled in the first visibility window and the NIRSpec observations in the second.

The study of MACSJ1149 will be a co-ordinated project with GTOs Massimo Stiavelli (NIRSpec R=1000 data) and Rogier Windhorst (NIRCам data). We will obtain the same data on this cluster as for our other targets because our data requirements differ from those of the other GTO teams. Multiple epochs of cluster imaging between the teams will be used to detect transients and increase depth. Some collaboration on projects with the other GTOs is expected, particularly on transients and NIRSpec target selection.

There is not space here to fully describe the data analysis plan. Our team includes world-leading experts in gravitational lens modeling, galaxy cluster imaging and photometry, WFC3 grism spectroscopy and multi-object spectroscopy. We plan to have a series of data challenges in the period 2017 to 2019 with simulated datasets processed by our reduction and analysis tools to ensure we are ready for the data when it arrives. Our aim is to make public high level data product releases within six months of the observation date of the NIRSpec data for each cluster. We will also likely release a small amount of NIRISS data even earlier to aid the GO community in their Cycle 2 proposal preparation and highlight the capabilities of NIRISS.

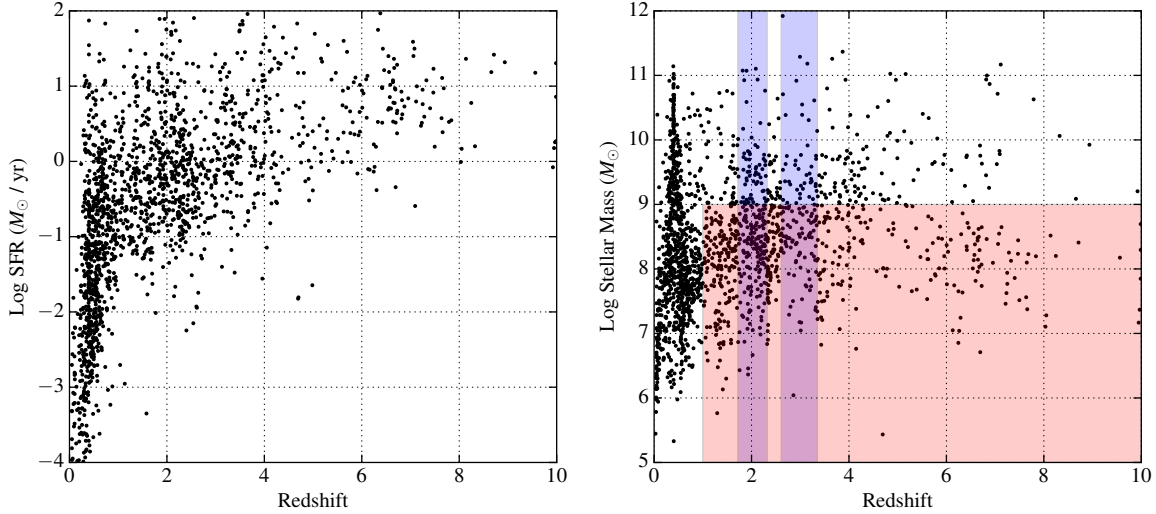


Figure 1: Demagnified (i.e. corrected for gravitational lensing) star formation rate (SFR; left) and stellar mass (right) as a function of redshift for galaxies brighter than $H_{AB} = 27.5$ in the Hubble Frontier Field cluster field MACS J0416 (Castellano et al. 2016). These plots illustrate the low SFR and mass of the galaxies that will dominate the NIRISS observations allowing us to determine the physics and evolution of low-luminosity and mass galaxies. The red shaded region shows the large number of $z > 1$ dwarf (stellar mass below $10^9 M_{\odot}$) galaxies. The blue shaded regions show the redshift ranges for NIRISS measurement of the emission lines to determine metallicities. The NIRISS GTO CANUCS survey will cover 5 such fields in order to measure properties of sufficient galaxies for our science cases and mitigate the effects of cosmic variance.

Figures and References

- | | |
|---|--|
| Castellano et al. 2016, A&A, 590A, 31 | Mannucci et al. 2010, MNRAS, 408, 2115 |
| Chardin et al. 2015, MNRAS, 453, 2943 | Momcheva et al. 2016, ApJS, 225, 27 |
| Dominguez et al. 2015, MNRAS, 451, 839 | Nelson et al. 2015, A&C, 13, 12 |
| Elmegreen & Elmegreen 2005, ApJ, 627, 632 | Oesch et al. 2016, ApJ, 819, 129 |
| Fumagalli et al. 2012, ApJ, 757L, 22 | Sanders et al. 2015, ApJ, 799, 138 |
| Genel et al. 2014, MNRAS, 445, 175 | Schenker et al. 2014, ApJ, 795, 20 |
| Genzel et al. 2008, ApJ, 687, 59 | Schmidt et al. 2016, ApJ, 818, 38 |
| Gilmore & Natarajan 2009, MNRAS, 396, 354 | Smit et al. 2014, ApJ, 784, 58 |
| Gnedin 2014, ApJ, 793, 29 | Stark et al. 2013, ApJ, 763, 129 |
| Guo et al. 2012, ApJ, 757, 120 | Steidel et al. 2014, ApJ, 795, 165 |
| Jauzac et al. 2016, MNRAS, 463, 3876 | Trenti & Stiavelli 2008, ApJ, 676, 767 |
| Jones et al. 2015, AJ, 149, 107 | van der Wel et al. 2011, ApJ, 742, 111 |
| Jullo et al. 2010, Science, 329, 924 | Wang et al. 2016, arXiv:1610.07558 |
| Ma et al. 2016, arXiv:1610.03498 | |

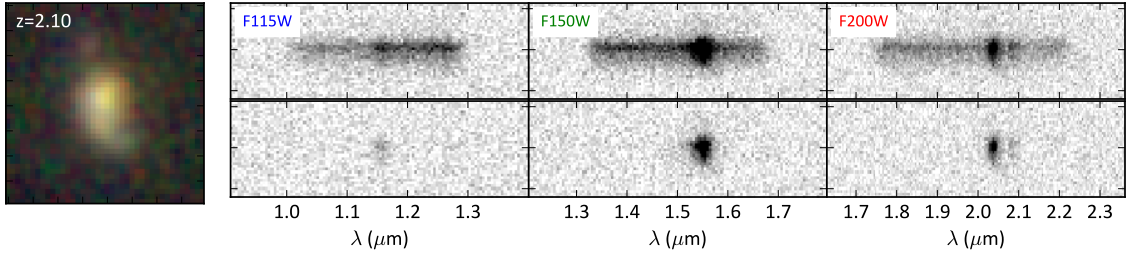


Figure 2: Simulated continuum-subtracted spectra of a line-emitting galaxy at $z \sim 2$. The lines shown in the three filters from left to right are [O II], $H\beta$ + [O III] and $H\alpha$ + [S II]. All line species are clearly detected and we will resolve the morphology and faint extended structures (e.g., tidal features) in the brighter lines.

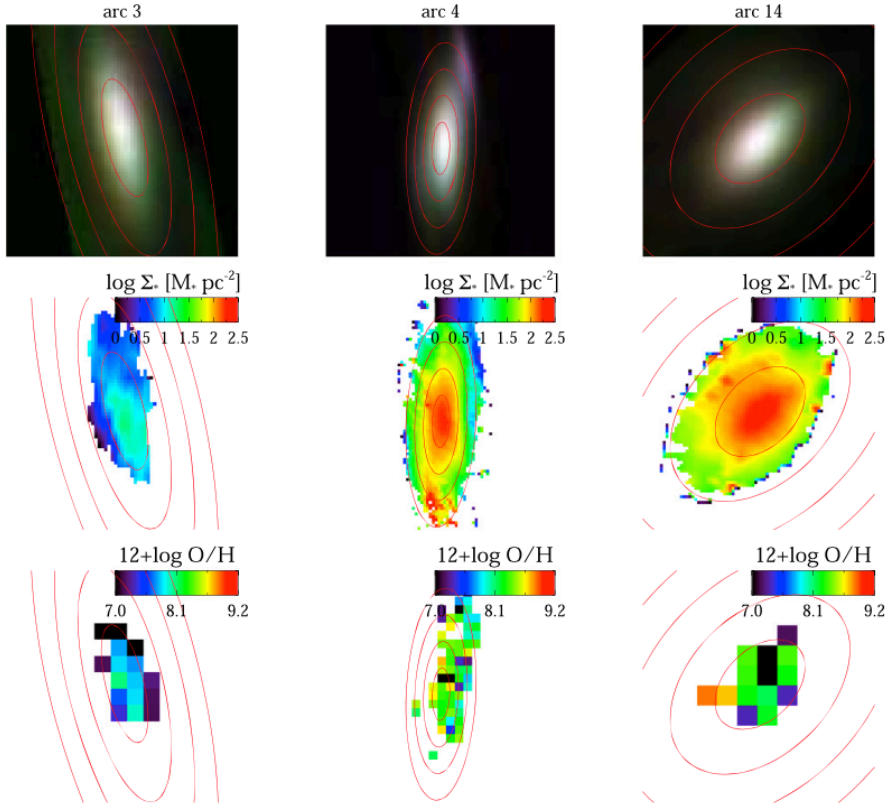


Figure 3: Reconstructed source plane images (upper), stellar mass maps (middle) and metallicity maps (lower) for three lensed arcs in a Frontier Fields cluster derived from *HST* grism data by the GLASS survey team (Jones et al. 2015). Arcs 3 and 14 are 2 kpc across and arc 4 is 8 kpc. With the vastly improved spatial resolution and sensitivity of NIRISS we will obtain high quality metallicity maps for ≈ 100 highly-magnified galaxies to study the competing effects of pristine gas infall and outflow of chemically enriched material.

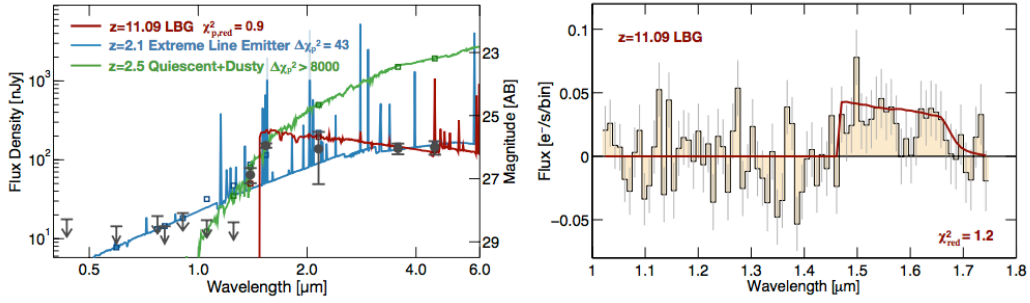


Figure 4: Left: SED for the highest redshift spectroscopically-confirmed galaxy at $z = 11.09$ showing the photometry is best fit by a high redshift solution. Right: The *HST* WFC3 G141 grism spectrum revealing a continuum break at $1.47\mu m$. From Oesch et al. (2016).

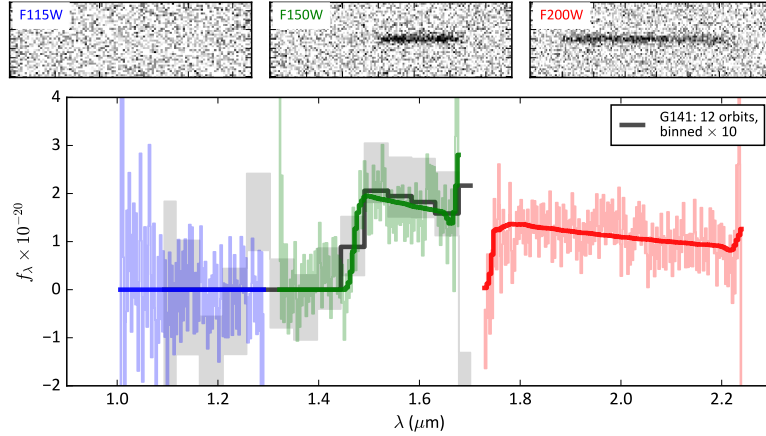


Figure 5: Simulation of the $z = 11$ galaxy in Fig. 4 for the proposed NIRISS observations. The spectrum redward of the Lyman break in the F150W filter is detected at $\sim 3\sigma$ per NIRISS spectral bin. There are only a handful of galaxies this bright at $z > 8$ in the cluster fields, but this demonstrates the dramatic increase in sensitivity and wavelength coverage of NIRISS.

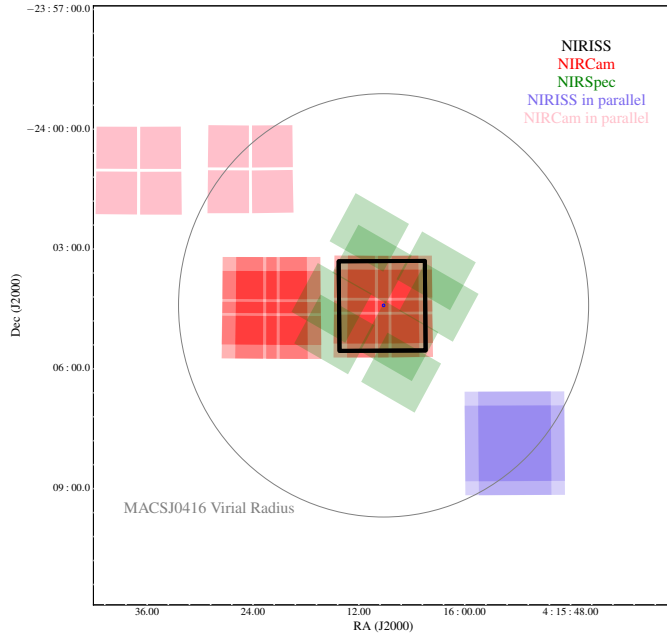


Figure 6: Relative instrument prime and parallel field locations for the CANUCS survey. The grey circle shows the virial radius of the cluster MACSJ0416 to highlight how these combined observations probe galaxies from the cluster core to the infall region.